Integrative Biology

PAPER

Single cell gene expression analysis in injury-induced collective cell migration†

Cite this: *Integr. Biol.*, 2014, 6, 192

Reza Riahi,[a] Min Long,[bc] Yongliang Yang,[a] Zachary Dean,[d] Donna D. Zhang,[be] Marvin J. Slepian[ef] and Pak Kin Wong*[ae]

Received 15th May 2013,
Accepted 24th November 2013

DOI: 10.1039/c3ib40095f

www.rsc.org/ibiology

Collective cell behavior in response to mechanical injury is central to various regenerative and pathological processes. Using a double-stranded locked nucleic acid probe for monitoring real-time intracellular gene expression, we examined the spatiotemporal response of epithelial cells during injury-induced collective migration and compared to the blocker assay with minimal injury as control. We showed that cells ~150 μm from the wound edge exhibit a gradient in response to mechanical injury, expressing different genes depending on the wounding process. While release of contact inhibition is sufficient to trigger the migratory behavior, cell injury additionally induces reactive oxygen species, Nrf2 protein, and stress response genes, including heat shock protein 70 and heme oxygenase-1, in a spatiotemporal manner. Furthermore, we show that Nrf2 has an inhibitory role in injury-induced epithelial–mesenchymal transition, suggesting a potential autoregulatory mechanism in injury-induced response. Taken together, our single-cell gene expression analyses reveal modular cell responses to mechanical injury, manipulation of which may afford novel strategies for tissue repair and prevention of tumor invasion in the future.

Insight, innovation, integration

Collective cell migration plays essential roles in developmental biology, regenerative medicine, and cancer metastasis. Using a double-stranded locked nucleic acid probe for monitoring intracellular mRNA in living cells, we study the spatiotemporal dynamics of intracellular gene expression in individual cells with different levels of injury during collective cell migration. This study reveals novel insights into modular responses of cells to mechanical injury and release of contact inhibition, and the inhibitory role of the Nrf2 signaling pathway in injury-induced epithelial–mesenchymal transition. These insights will guide future investigations of injury-induced cell responses and may lead to novel therapeutic strategies in the future.

Introduction

Collective cell migration is a fundamental multicellular activity that plays essential roles in numerous physiological and pathological processes, such as embryogenesis, tissue regeneration, and cancer metastasis.[1–3] Proper coordination of epithelial cells is required to repair damaged tissue, in which cells crawl collectively atop an exposed extracellular matrix following injury.[4] Similarly, collective cell migration of endothelial and smooth muscle cells is vital in vascular tissue repair following injury, *e.g.* post-angioplasty.[5,6] The collective migration mechanisms responsible for embryogenesis and tissue repair are also utilized in invasion and metastasis of malignant tumors.[7] For example, collective invasion of squamous cell carcinomas, which are of epithelial origin and have intact E-cadherin based junctions, in the form of protruding strands are often observed in histopathological analyses. In addition to sheets and strands that maintain contacts with the primary tumor, other morphological and functional variants such as detached cells or cell clusters are also observed. In particular, cancer cells can undergo epithelial–mesenchymal transition (EMT) and detach from the primary tumor to migrate individually or collectively.[8–10] During EMT, epithelial cells lose cell–cell contact and planar polarity, and

[a] *Department of Aerospace and Mechanical Engineering, The University of Arizona, Tucson, Arizona 85721, USA. E-mail: pak@email.arizona.edu; Fax: +1-520-621-8191; Tel: +1-520-626-2215*
[b] *Department of Pharmacology and Toxicology, The University of Arizona, Tucson, AZ 85721-0119, USA*
[c] *Department of Endocrinology, Xinqiao Hospital, Third Military Medical University, Chongqing 400037, PR China*
[d] *Biomedical Engineering Interdisciplinary Program, The University of Arizona, Tucson, AZ 85721-0119, USA*
[e] *BIO5 Institute, The University of Arizona, Tucson, AZ 85721-0119, USA*
[f] *Department of Medicine, The University of Arizona, Tucson, AZ 85724, USA*

† Electronic supplementary information (ESI) available: Data showing experimental approaches of wound healing assays, expression of Nrf2 by SFN, and, immunostaining results for different cell phenotypes. See DOI: 10.1039/c3ib40095f

acquire a mesenchymal phenotype, which has high motility and invasiveness. In contrast to the classical view, collective cell migration is also suggested to be a fine-tuned, partial EMT process, in which cells near the leading edge undergo different degrees of EMT to enable efficient migration of the cohesive epithelia while maintaining internal organization.[11,12]

Understanding injury-induced collective migration and the ability to modulate this complex process may have a profound impact on translational medicine. For instance, emerging evidence has indicated that tissue biopsy and surgical removal of primary tumors may induce cell injury and increase the potential of metastatic tumor outgrowth, as well as the circulating tumor cell count.[13–17] However, injury-induced cell migration processes are challenging to study, as only a small amount of cells near the wound are responding to the injury, and numerous interrelated molecular and signaling events are involved. For instance, it is known that cell injury induces the reactive oxygen species (ROS) level during wound healing and ROS production can trigger the EMT process.[18,19] It has also been proposed that EMT can be modulated by the nuclear factor E2-related factor 2 (Nrf2) signaling pathway.[20] Recently, Nrf2 has been demonstrated to suppress EMT in cyclosporin A-induced renal fibrosis and reduce the invasiveness of cancer cells.[21,22] Nevertheless, the involvement of Nrf2 in the injury response and the potential role of Nrf2 in injury-induced EMT have not been explored. Systematic investigations are required to decipher what influence mechanical injury has on cells, how many cells are involved, and how cells regulate the injury response during collective migration.

Elucidating the collective cell behaviors, nevertheless, is hindered by a lack of effective approaches for monitoring the individual cell responses during injury-induced collective cell migration. While single-cell measurement techniques such as microfluidics and single-cell PCR platforms exist, these techniques often disrupt the cell organization and cannot monitor the dynamics of cell behaviors.[23,24] To address this challenge, minimally-invasive biosensing techniques with high spatiotemporal resolution are required. We have previously developed a homogeneous biosensor, double-stranded DNA, which binds rapidly to a specific nucleic acid sequence and produces a fluorescence signal.[25–27] By modifying the probe with locked nucleic acid monomers to enhance its intracellular stability and specificity, the double-stranded locked nucleic acid (dsLNA) probes enable us to measure the dynamics of intracellular gene expression in living cells over an extended period of time.[28]

In this study, the effect of mechanical injury on collective cell migration of epithelial cells was investigated. To separate the effects of cell injury and release of contact inhibition, the scratch assay and polydimethylsiloxane (PDMS) assays, which introduced different levels of cell injury, were employed. The spatiotemporal response of cells was monitored by the intracellular dsLNA probes and other molecular assays. The expression of several migratory and stress response genes, including β-actin, heme oxygenase-1 (*HO-1*) and heat shock protein 70 (*HSP70*), was monitored in cells near the wound by the dsLNA probes. The cell migration rate, the ROS level, and the Nrf2 protein level were also measured and compared between the two wounding assays. Furthermore, the inhibitory effect of Nrf2 on injury-induced EMT was studied by modulating the activity of Nrf2 with sulforaphane (SFN) and siRNA targeting Nrf2.

Materials and methods

Reagents and cell culture

Unless otherwise specified, all chemicals were purchased from Sigma (Saint Louis, MO, USA). Synthetic targets and dsLNA probes were synthesized by Integrated DNA Technologies Inc. The Nrf2 siRNA and the control siRNA were purchased from Qiagen (Valencia, CA, USA). The effectiveness and specificity of the siRNA have been tested previously.[29,30] Breast cancer cell lines, MCF7 and MDA-MB-231, were obtained from the ATCC (Manassas, VA, USA). Cells were maintained in Dulbecco's modified Eagle's medium (DMEM) from Invitrogen (Carlsbad, CA, USA) supplemented with 10% fetal bovine serum, 2 mM HEPES buffer, and 0.1% gentamycin at 37 °C and 5% CO_2. Cells were plated in 24-well tissue culture plates or glass coverslips placed in six-well plates. To form uniform epithelia for wound healing experiments, cells were seeded at an initial concentration of 10^5 cell per ml for 2 days.

Establishment of a Nrf2-YFP stable cell line

The Nrf2-YFP plasmid has been previously described.[31] The Nrf2-YFP plasmid was transfected into MDA-MB-231 cells using Lipofectamine Plus from Invitrogen (Grand Island, NY, USA), according to the manufacturer's instructions. At 48 hours post-transfection, cells were grown in medium containing 800 μg ml^{-1} G418 from Cellgro (Manassas, VA, USA) for selection. Stable cell lines were established after all cells in the negative control plate were killed. Single colonies were picked and were continuously grown in the DMEM medium containing 600 μg ml^{-1} G418. The stable cell lines were evaluated by immunoblot and fluorescence microscopy.

Wound-healing assays

Cells were incubated in serum-free culture media for 30 minutes prior to wounding. Two wounding assays were utilized (Fig. 1a and b and Fig. S1a, ESI†). For the scratch assay, a model wound was created by scrapping in the middle of the confluent cell monolayer with a sterilized 1000 μl pipette tip. To create an empty space for cell migration with minimal injury, the PDMS assay was utilized.[32–35] PDMS was prepared at a 10 : 1 precursor/curer ratio, poured into a 100 mm petri dish to 2 mm height, and baked for 3 hours at 70 °C. Blocks of PDMS (5 mm × 2 cm) were cut with a razor, sterilized with ethanol, and incubated in 3% heat denatured bovine serum albumin (BSA) dissolved in PBS for 1 hour. The PDMS slab was placed onto a 24 well plate forming conformal contact with the surface, which was required to prevent cells from entering into the space under the PDMS slab. After a confluent cell monolayer was formed, the slab was removed, effectively unconstraining the cells. The PDMS lift-off process was performed carefully to minimize the mechanical stress on the cell boundary.

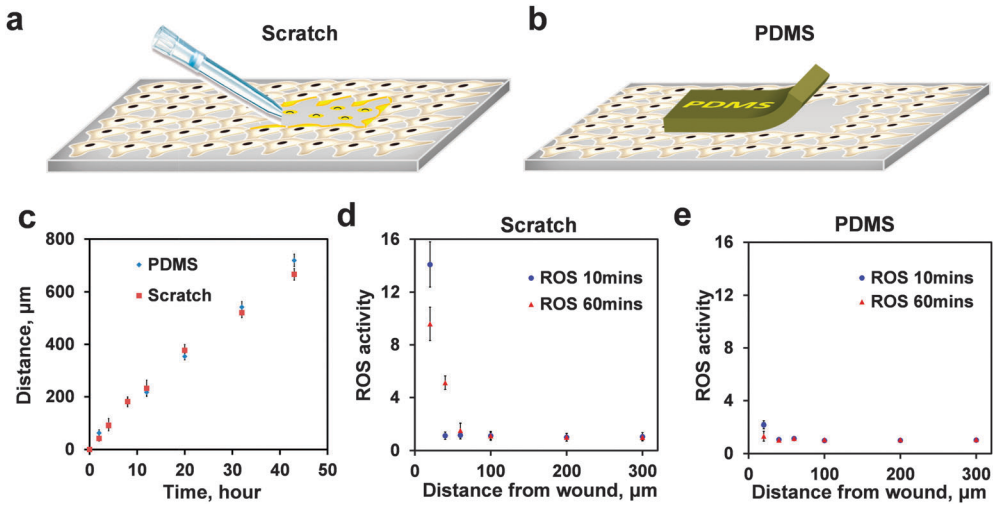

Fig. 1 Coordinated responses of epithelial cells when encountering mechanical injury. (a and b) Schematics of two wound healing assays that introduce different degrees of cell injury. In the scratch assay, a pipette tip is applied to physically scrap an intact monolayer to introduce a model wound. In the PDMS assay, a PDMS slab is placed on a tissue culture dish or a glass coverslip before cell seeding. By lift-off the PDMS slab, the assay allows release of contact inhibition to induce collective cell migration with minimum cell injury. (c) The displacement of the wound leading edge in the scratch and PDMS assays at different time points. (d and e) Distribution of the ROS level near the wound after mechanical scratching and PDMS lift-off.

Probe design and preparation

The dsLNA probe is a homogeneous assay for detecting specific nucleic acid sequences.[25–28] The LNA probe contains a fluorophore labeled on the 5′ end and is designed to be complementary to the target mRNA (Fig. S1b, ESI†). A complementary quencher probe is also designed with respect to the fluorophore probe. The 3′ end of the quencher probe is conjugated with a quencher. In the absence of a target mRNA, the fluorophore and quencher probes are in close proximity, diminishing the fluorescence signal. With a target, the quencher probe is replaced by the mRNA due to the thermodynamically-driven hybridization event between the fluorophore probe and the target. As a result, the fluorophore is separated from the quencher and fluoresces. To resist nuclease digestion and avoid non-specific binding with DNA binding proteins, alternating LNA/DNA monomers were used. Alternating LNA/DNA was shown to balance between probe stability and sensitivity.[28] In this study, three different probes were designed based on β-actin, *HO-1*, and *HSP70* mRNA sequences (Table 1). A random probe was also designed as negative control. The target sequences were obtained from NCBI GenBank and the probe sequences were designed using Mfold and NCBI Basic Local Alignment Search Tool (BLAST).[36,37] Before transfections, the dsLNA probes were prepared by mixing fluorophore and quencher probes at a 1-to-2 ratio. After 5 min incubation in a water bath at 95 °C, the dsLNA probes were cooled down for 3 hours to reach room temperature.

Gene expression measurement using dsLNA probes

Cells were plated in 24-well plates for 24 hours. The cells were transfected with a 0.8 μg dsLNA probe using lipofectamine 2000 in opti-MEM (Invitrogen, Grand Island, NY, USA). The scratch and PDMS wounding assays were performed 24 hours after transfection. The cells exhibited similar behaviors with and without the probes. This observation is consistent with previous intracellular probe studies.[38] Furthermore, the dsLNA probes were applied only in the mRNA expression experiments and have no effect on other molecular and migratory assays.

Visualization of ROS near the wounds

The fluorescent indicator 5-(and-6)-chloromethyl-2′,7′-dichlorodihydrofluorescein diacetate, acetyl ester (CM-H2DCFDA) from Invitrogen (Carlsbad, CA, USA) was utilized to visualize the ROS level. This dye readily diffuses into cells and starts to fluoresce due to intracellular removal of acetate groups of CM-H2DCFDA in the presence of ROS. Shortly before the experiment, the dye was diluted to a stock solution of 1000 μM in anhydrous DMSO.

Table 1 Probe sequences applied in this study. The probes were designed to have alternating LNA/DNA monomers. Crosses (+) indicate LNA monomers

Probe type	Label	Sequence	Length, bases
β-Actin donor	5′ FAM-6	5′-/+AG+GA+AG+GA+AG+GC+TG+GA+AG+AG/-3	20
HO-1 donor	5′ FAM-6	5′-/+AA+GA+CT+GG+GC+TC+TC+CT+TG+TT/-3′	20
Hsp70 donor	5′ FAM-6	5′-/+TT+GT+CG+TT+GG+TG+AT+GG+TG+AT/-3′	20
Random quencher	5′ FAM-6	5′-/+AC+GC+GA+CA+AG+CG+CA+CC+GA+TA/-3′	20
β-Actin quencher	3′ Iowa Black RQ™	5′-/+CT+TC+CT+TC+CT/-3′	10
HO-1 quencher	3′ Iowa Black RQ™	5′-/+GC+CC+AG+TC+TT/-3′	10
Hsp70 quencher	3′ Iowa Black RQ™	5′-/+CC+AA+CG+AC+AA/-3′	10
Random quencher	3′ Iowa Black RQ™	5′-/+CT+TG+TC+GC+GT/-3′	10

Cells were pre-incubated with 5.0 μM dye (final concentration) diluted in phenol red-free DMEM for 30 min at 37 °C. To measure the ROS induced by ATP and cell lysate, cells were seeded at a density of 40 000 cells per cm^2, incubated for 24 hours, and exposed to cell lysate or 100 μM ATP. Then, 5 μM dye (final concentration) was added for 30 minutes before measuring the signal.

Immunofluorescence staining assay

Cells were fixed using 3.7% formaldehyde for 15 minutes at room temperature. Immunostaining was performed 48 hours after the wounding assays. Permeabilization was achieved by incubating 0.1% Triton X-100 for 10 minutes at room temperature. After blocking with 1% BSA in PBS for 30 minutes, cells were incubated for 60 minutes with the Alexa 488 conjugated anti-vimentin antibody from Santa Cruz Biotechnology (Santa Cruz, CA, 1 : 100 dilution), the Alexa 555 conjugated anti-E-cadherin antibody from BD Biosciences (San Jose, CA, 1 : 100 dilution), and rhodamine–phalloidin from Invitrogen (Carlsbad, CA, 1 : 40 dilution). For other proteins, cells were incubated with primary antibodies against vinculin from Sigma (St. Louis, MO, 1 : 400 dilution), and Sanil and N-cadherin from Santa Cruz Biotechnology (Santa Cruz, CA, 1 : 100 dilution). The primary antibodies were detected by anti-mouse Alexa Fluor 488-, or anti-mouse or anti-rabbit Alexa Fluor 555-conjugated secondary IgG antibodies from Invitrogen (Carlsbad, CA, 1 : 500 dilution). Then, the 4′,6-diamidino-2-phenylindole (DAPI) antifade reagent from Invitrogen (Carlsbad, CA, USA) was added to the sample for nuclear staining.

Nrf2 measurement and small interfering RNA

Scratch and PDMS assays were performed for the Nrf2-YFP and control YFP stable cell lines. The fluorescence signals were monitored for 3 days after wounding. Nrf2 siRNA and control siRNA were purchased from Qiagen (Valencia, CA, USA). Transfection of siRNA was performed using the HiPerFect Transfection Reagent according to the manufacturer's protocol (Qiagen). A concentration of 20 nM siRNA was applied 48 hours prior to mechanical injury. For SFN, a concentration of 5.0 μM was incubated with the cell monolayer for 12 hours before wounding. Cells were stained 48 hours after wounding.

Immunoblot analysis

Cell lysates were prepared as previously described.[39,40] Protein concentration was determined using the Quant-IT Protein Assay kit (Invitrogen). Cultured cells were lysed in sample buffer (50 mmol L^{-1} Tris-HCl [pH 6.8], 2% SDS, 10% glycerol, 100 mmol L^{-1} dithiothreitol, 0.1% bromophenol blue). Total lysates were loaded and electrophoresed through SDS–polyacrylamide gels for immunoblot analysis.

Microscope image acquisition

For dsLNA assays, live cells were monitored using an inverted fluorescence microscope (TE2000-U, Nikon, Japan). Bright-field and fluorescence images were acquired using a CCD camera (SensiCamQE, Cook corp., Romulus, MI, USA) at different time points for three days. For immunofluorescence staining, fluorescence images were captured using a HQ2 CCD camera (Photometric, Tucson, AZ, USA). Images were taken under the same conditions for comparison. The exposure times were 0.5 s and 1 s for the immunostaining and dsLNA experiments, respectively. Data collection and imaging analysis were performed using the NIH ImageJ software. For dsLNA probe measurement, the intensity in the cytoplasm of each individual cell was measured and reported in arbitrary units.

Statistical analysis

Student *t* tests were performed to compare between experimental groups. For intensity measurements in Nrf2-YFP and dsLNA assays, each data point represents mean ± SEM of at least 30 cells near the wound edges in the PDMS and scratch assays. Data represent mean ± SEM. All experiments were repeated for at least three times (n = 3–5).

Results

Release of contact inhibition is sufficient to induce collective cell migration

Two wounding approaches, the scratch assay and the PDMS assay, were applied to study the effects of mechanical injury on collective cell migration. For the scratch assay, cells were mechanically scraped off the tissue culture plate. To separate the effects of cell injury from those induced by the release of contact inhibition, the PDMS assay, associated with a reduced amount of cell injury, was utilized. Specifically, a PDMS slab was placed on the tissue culture plate before cell seeding and the slab was removed to create unconstrained space for cell migration. Similar techniques have been described for studying the effects of release of contact inhibition on cells.[32–35] In our experiment, we first compared the effects of these wounding strategies on cell migration. The position of the leading edge was observed to increase linearly with time and the migration rates were approximately the same for both assays (Fig. 1c). This observation is in agreement with previous studies using injury-free wounding assays that the release of contact inhibition is sufficient to induce collective cell migration.[32–35]

Cell injury induces ROS and Nrf2 near the wound

ROS, which are known to involve in wound healing, were investigated.[19,20] We monitored and compared the distribution of ROS in the scratch and PDMS assays (Fig. 1d and e). Upon scratching, the ROS level first increased in the leading edge. Then, the ROS level appeared to propagate to the adjacent rows of cells ~100 μm from the wound edge. A high level of ROS was observed at the wound edge 10 minutes after wounding and the increase in the ROS level lasted over 60 minutes. In contrast, only a low level of ROS was observed near the wound in the PDMS assay. These observations suggest that the release of contact inhibition alone does not trigger ROS generation and release, rather cell injury is required for the elevation of ROS.

A key regulator of ROS is the transcription factor Nrf2, which mediates many antioxidant and stress response genes through

interactions with the antioxidant response element.[20] Nrf2 is primarily controlled at the protein level. To elucidate the involvement of Nrf2 in injury-induced wound healing, we established a Nrf2-YFP stable cell line and a control YFP cell line for monitoring the Nrf2 protein level in the wounding assays. We first examined the Nrf2-YFP stable cell line using immunoblot and fluorescence microscopy (Fig. S2, ESI†). By incubating 5 μM SFN with the cells, the Nrf2 protein level was increased and nuclear accumulation of the Nrf2-YFP protein was observed. Then, the cells were applied in the scratch and PDMS assays (Fig. 2 and Fig. S3, ESI†). In the scratch assay, the intensity near the wound edge was increased in the Nrf2-YFP cells, but not in the control YFP cells. Interestingly, Nrf2 was upregulated at two different time points after wounding. The first peak was relatively low, peaking between 3–4 h after wounding. The second peak was higher, peaking at ~24 h. Furthermore, the spatial distribution of Nrf2 in the scratch assay correlated with the ROS level. In particular, cells within 100–150 μm from the leading edge showed an increase in the Nrf2-YFP level. In contrast, the Nrf2 intensity was roughly constant in the PDMS assay throughout the duration of the experiment. For the PDMS assay, the intensities could not be distinguished between control YFP and Nrf2-YFP cells. These observations reveal that Nrf2 can be induced in cells near the wound by mechanical injury, but not *via* the release of contact inhibition alone.

Spatiotemporal gene expression profiles

To characterize the cellular responses triggered by cell injury, the level of β-actin mRNA, which can be induced by mechanical injury, was studied.[41] *HO-1* (a downstream gene of Nrf2) and *HSP70* (a stress response gene) were also included to elucidate the roles of mechanical injury in the cellular stress response. These genes are known to have cytoprotective roles in wound healing.[18,42] To monitor the expressions in living cells, dsLNA probes were first transfected into the cells (Fig. 3a). The intracellular gene expression distribution was measured in the scratch and PDMS assays (Fig. 3b). Examining the intensity distribution revealed a gradient of β-actin mRNA near the wound (Fig. 3c). The intensity at the leading edge was almost 3-fold higher than the values in cells far away from the wound. The intensities dropped gradually from the leading edge toward the inner region of the cell monolayer, reaching a low level at approximately 150 μm. The intensity and spatial distributions for β-actin were similar in the scratch and PDMS assays (Fig. 3d). This observation was consistent with the migration rate data, which indicated that the release of contact inhibition is sufficient to induce the cellular migratory response. In addition,

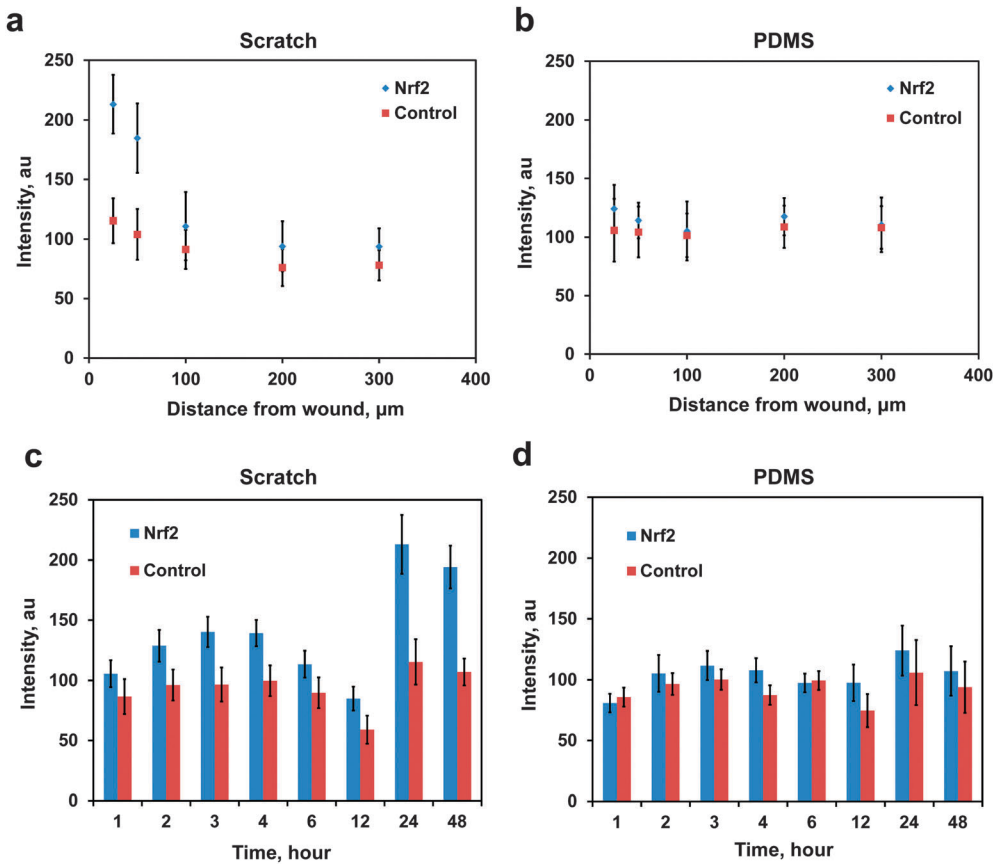

Fig. 2 Spatiotemporal distributions of Nrf2 protein in the scratch and PDMS assays. (a) Spatial distribution of the Nrf2-YFP intensity at 24 hours after the scratch assay. (b) Spatial distribution of the Nrf2-YFP intensity at 24 hours after the PDMS assay. (c) Dynamics of the Nrf2-YFP intensity at the wound edge after the scratch assay. (d) Dynamics of the Nrf2-YFP intensity at the wound edge after the PDMS assay.

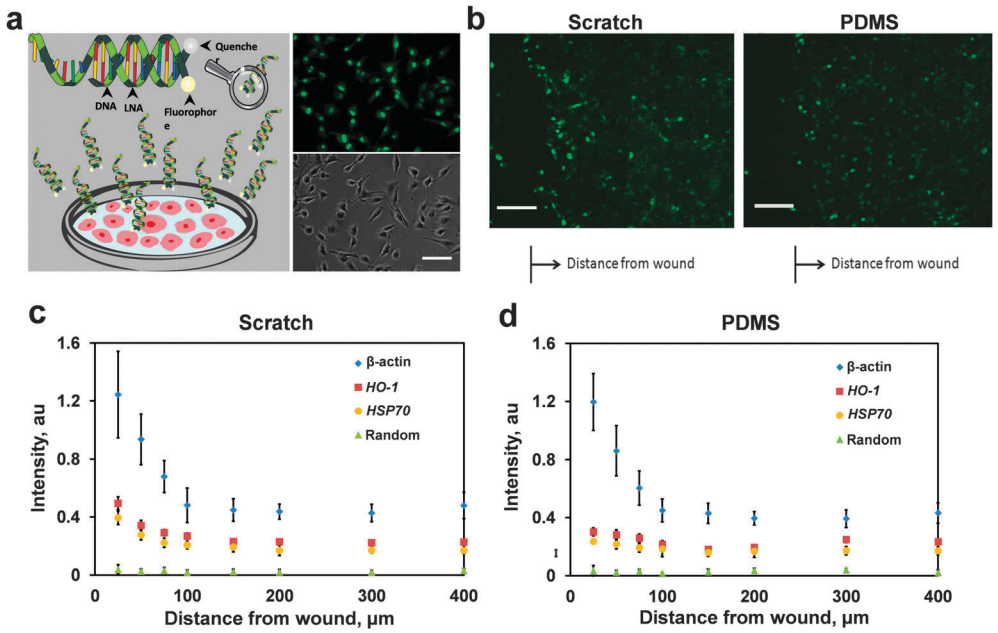

Fig. 3 Intracellular gene expression measurement of individual cells near the model wounds by transfecting dsLNA probes to the cells. (a) The design of the dsLNA probe consisting of alternative DNA and LNA monomers to enhance the probe stability for intracellular detection. The probe can be transfected to cells with a high efficiency for monitoring the cell responses near the wound. Images on the right hand side show fluorescence and bright field images of cells transfected with β-actin probes in MDA-MB-231 cells. The images were obtained 24 hours after probe transfection. (b) Intracellular gene expression of *HO-1* mRNA in MCF7 cells observed in the (left) scratch and (right) PDMS assays. Images were taken 48 hours after wounding. Scale bars, 100 μm. (c and d) Spatial distribution of gene expression of MCF7 cells near the wound. β-Actin, *HO-1*, *HSP70*, and random probes were transfected to cells for 24 hours before (left) mechanical scratching and (right) PDMS lift-off.

the intensities of *HO-1* and *HSP70* mRNAs at the leading edge were at least 2-fold higher than the values in cells in the inner region with the scratch assay. Similar to β-actin, the intensity dropped from the leading edge toward the inner region of the cell monolayer and the values reached the basal level at approximately 150 μm from the wound edge. In contrast, relatively uniform distributions of *HO-1* and *HSP70* mRNA were observed in the PDMS assay. The levels of *HO-1* and *HSP70* mRNAs at the wound edge were significantly higher than the values in the PDMS assay.

We have also measured the gene expression dynamics after wounding. The levels of β-actin and *HO-1* mRNA continuously increased in the first three days in both scratch and PDMS assays (Fig. 4a and b). In contrast, the *HSP70* mRNA reached the maximum level two days after wounding (Fig. 4c), which is consistent with previous studies in rabbit cornea.[43] For *HO-1* and *HSP70*, the intensities in the scratch assay were significantly higher than the values obtained in the PDMS assay at different time points. As a control, the intensity of the random control probe was at a low level throughout the experiment (Fig. 4d). Collectively, the data suggest that release of contact inhibition can trigger the β-actin expression while cell injury is required for inducing the stress response genes including *H0-1* and *HSP70*.

Injury-induced EMT

Detected cells and clusters with migratory phenotypes were observed in the scratch assay. We hypothesized that cell detachment and the migratory phenotypes, which are characteristics of EMT, were triggered by mechanical injury. We first measured the expressions of epithelial and mesenchymal biomarkers, including E-cadherin and vimentin, in both intact MCF7 and MDA-MB-231 monolayers (Fig. S4, ESI†). In the scratch assay (Fig. 5a), MCF7 cells detached from the monolayer and near the wound showed a reduced level of E-cadherin with an increase in vimentin compared to the intact monolayer. Interestingly, some cells in the cluster had low levels of vimentin and migrated along with cells having high levels of vimentin. For the PDMS assay, only minor changes in the E-cadherin and vimentin levels near the wound were observed (Fig. 5b). The cells near the wound were also characterized with other mesenchymal biomarkers, including N-cadherin, and Snail (Fig. 6a and b).[44,45] The detached cells increased their expressions of mesenchymal biomarkers and reduced the E-cadherin expression. Immunoblot analysis further confirmed that Snail was upregulated in the scratch assay (Fig. S5a, ESI†). Then, we characterized the morphology of cells near the wound. Fig. 6c–e illustrated F-actin and vinculin staining in the scratch assay, PDMS assay, and the intact monolayer. In the scratch assay, cells showed reorganization of actin cytoskeleton and formation of focal adhesion near the wound edge. In particular, detached cells had irregular shapes and exhibited well-defined actin stress fibers and focal adhesion. In the PDMS assay, cells near the wound edge also displayed morphological changes and formation of focal adhesion. Few detached cells were observed. In contrast, cells in the monolayer were packed and exhibited cortical actin filaments.

We quantified the number of detached cells and clusters to compare the effects of the wounding assays. In general, a larger

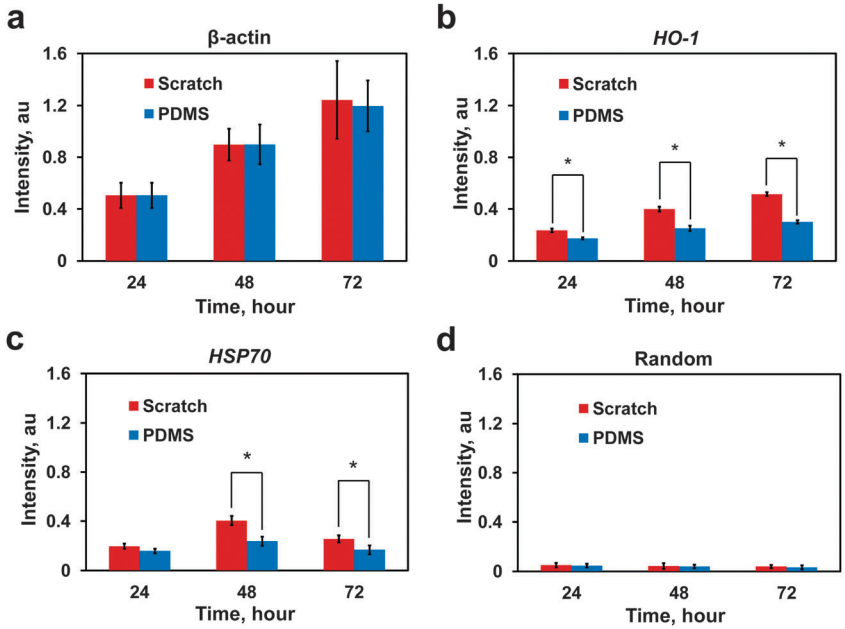

Fig. 4 Dynamics of intracellular mRNA expression. Intensities of (a) β-actin, (b) *HO-1*, (c) *HSP70*, and (d) random probes in MCF7 cells at the leading edge. Time is the duration after scratching of the monolayers or removal of the PDMS slabs. (* $P < 0.05$ compared between scratch and PDMS assays).

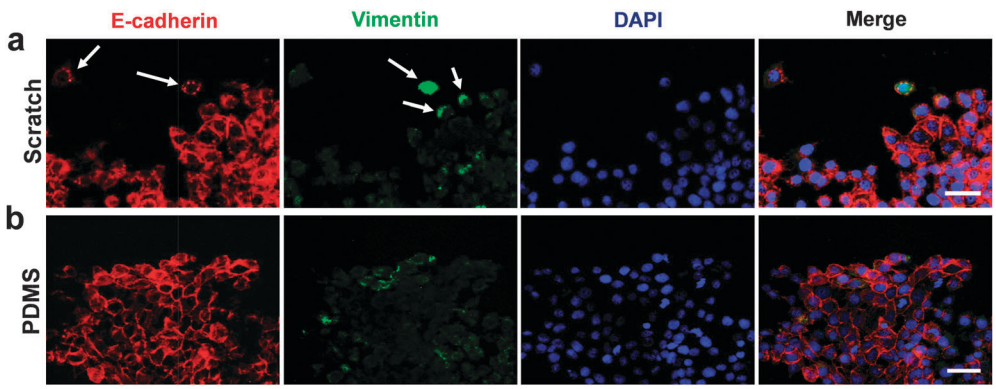

Fig. 5 Injury-induced EMT. Comparison of the phenotypes of MCF7 cells in the (a) scratch and (b) PDMS assays. 48 hours after performing wound healing assays cells were stained with E-cadherin and vimentin monoclonal antibodies conjugated with Alexa 555 and Alexa 488 fluorophores respectively. DAPI was used as counterstain. Detached cells or cell clusters were monitored (white arrows). Scale bars, 50 μm.

number of detached cells were observed in the scratch assay. As shown in Fig. 7, the number of detached cells in the scratch assay was three times higher than the value in the PDMS assay. This observation correlated with the loss of E-cadherin in the scratch assay compared to the PDMS assay. Live cell imaging experiments were performed to confirm that the detached cells were migrated from the monolayers during collective migration. We also quantified the number of detached cells with biomarkers of interest. In both assays, only a small portion of detached cells expressed E-cadherin and the majority displayed mesenchymal biomarkers, in particular for vinculin-based focal adhesion and Snail protein.

Inhibitory role of Nrf2 in injury-induced EMT

To determine the role of Nrf2 in injury-induced EMT, we modulated the Nrf2 activity by Nrf2 siRNA and SFN in the wounding assays using MCF7 cells. The activity of the Nrf2 siRNA was evaluated by immunoblot (Fig. S5b, ESI†). In the experiments, suppression of Nrf2 reduced E-cadherin and increased vimentin expressions in the scratch assay (Fig. 8a and Fig. S6, ESI†). The cells appeared to lose cell–cell contact, detach from each other, acquire an invasive phenotype, and migrate toward the wound site. An increase in the cell migration rate was also observed (Fig. S7, ESI†). Inducing the Nrf2 activity by SFN, in contrast, showed an increase in E-cadherin and reduction in vimentin (Fig. 8b). Cells also maintained the cell–cell contact. Transfecting the control siRNA has no observable effect (Fig. 8c). Similar effects of Nrf2 on the EMT biomarkers, cell–cell contact, and cell migration were also observed in the PDMS assay (Fig. 8d–f). The effects of Nrf2 were further studied by counting the detached cells (Fig. 9a). The results showed inducing Nrf2 suppressed injury-induced cell detachment and Nrf2 knockdown resulted in cell detachment in

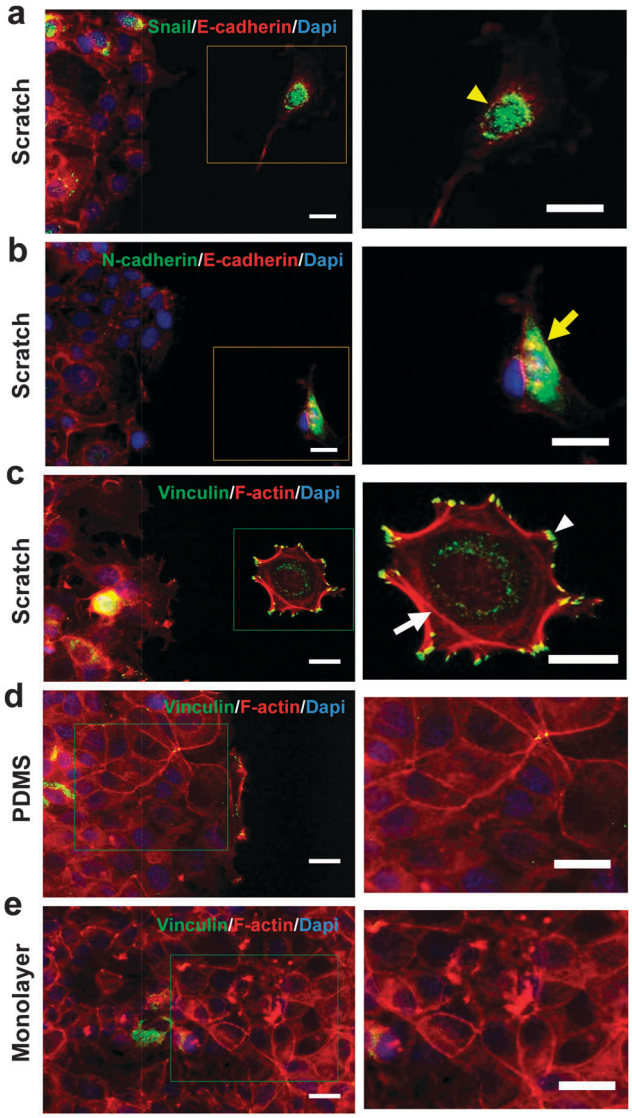

Fig. 6 Characterization of EMT biomarkers and cell morphology. (a and b) MCF7 cells near the wound edge in the scratch assay were evaluated by immunostaining of mesenchymal and epithelial biomarkers including Snail, N-cadherin, and E-cadherin. Yellow arrowhead and yellow arrow indicate detached cells with increased Snail and N-cadherin, respectively. (c–e) Immunostaining of F-actin and vinculin for cells in the scratch assay, PDMS assay and monolayer. White arrow and arrowhead indicate stress fibers and focal adhesion structures. DAPI was used as counterstain. Boxes indicate the magnified views shown on the right. Scale bars, 25 μm.

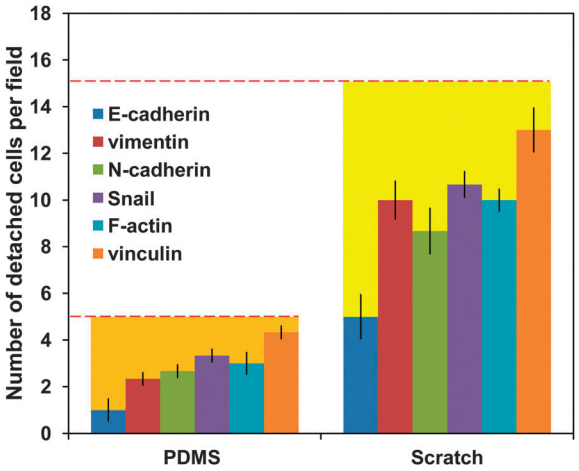

Fig. 7 Quantification of the number of detached cells in the PDMS and scratch assays. MCF7 cells were tested in the experiment. Dashed lines indicate the average number of detached cells per field in the PDMS and scratch assays. Each bar represents the average number of detached cells with the biomarker. The biomarkers were characterized by immunostaining. For F-actin and vinculin, only cells displaying well-defined stress fibers and focal adhesion were counted. The field of view of the images is 1 mm × 1 mm.

both wounding assays. These results suggested an inhibitory role in cell detachment and EMT. Immunoblot further supported the inhibitory role of Nrf2 in EMT (Fig. 9b). In particular, Nr2f suppression resulted in an increase in Snail while Nrf2 induction led to reduction in Snail protein. Collectively, these results supported the inhibitory role of Nrf2 in injury-induced EMT.

Discussion

In this study, we systematically investigated how epithelial cells respond to mechanical injury. The influences of cell injury were separated from contact inhibition *via* utilization of the scratch and PDMS assays, which introduce differing levels of cell injury. We demonstrated that cell injury upregulates the stress response genes, including *HO-1* and *HSP70*, and triggers EMT in cells near the wound edge. Remarkably, release of contact inhibition using the PDMS assay has only minor effects on the stress response genes. We, however, do not rule out the possibility of EMT induction by the release of contact inhibition, since detached cells and morphological changes were also observed in the PDMS assay. These observations suggest that the migratory and injury behaviors are different modularities in the cellular response program. This modular control may represent an effective, adaptable strategy for cells to manage different situations, since the stress responses may not be required in some normal physiological scenarios, such as tissue development. Another implication of the modular control is the selection of experimental approaches for investigating collective cell migration. Recently, numerous wounding assays, including physical, solid/liquid barrier, chemical removal, microfluidic, electrical and optical wounding, have been developed.[3] In particular, several injury-free assays have been proposed.[32–35] These injury-free assays, such as the PDMS assay, have several advantages including repeatable, compatible to geometric control, high throughput, and easy to use. Nevertheless, the role of cell injury should be considered when the migration processes being studied involve damage tissue repair and EMT. It may be best to perform multiple wound healing assays in parallel to avoid ambiguity in interpretation of the results.

To determine the spatiotemporal response of cells, we developed dsLNA probes for monitoring gene expression in individual cells near the wound. In the scratch assay, the cells display active, gradient responses in β-actin, *HO-1*, and *HSP70*

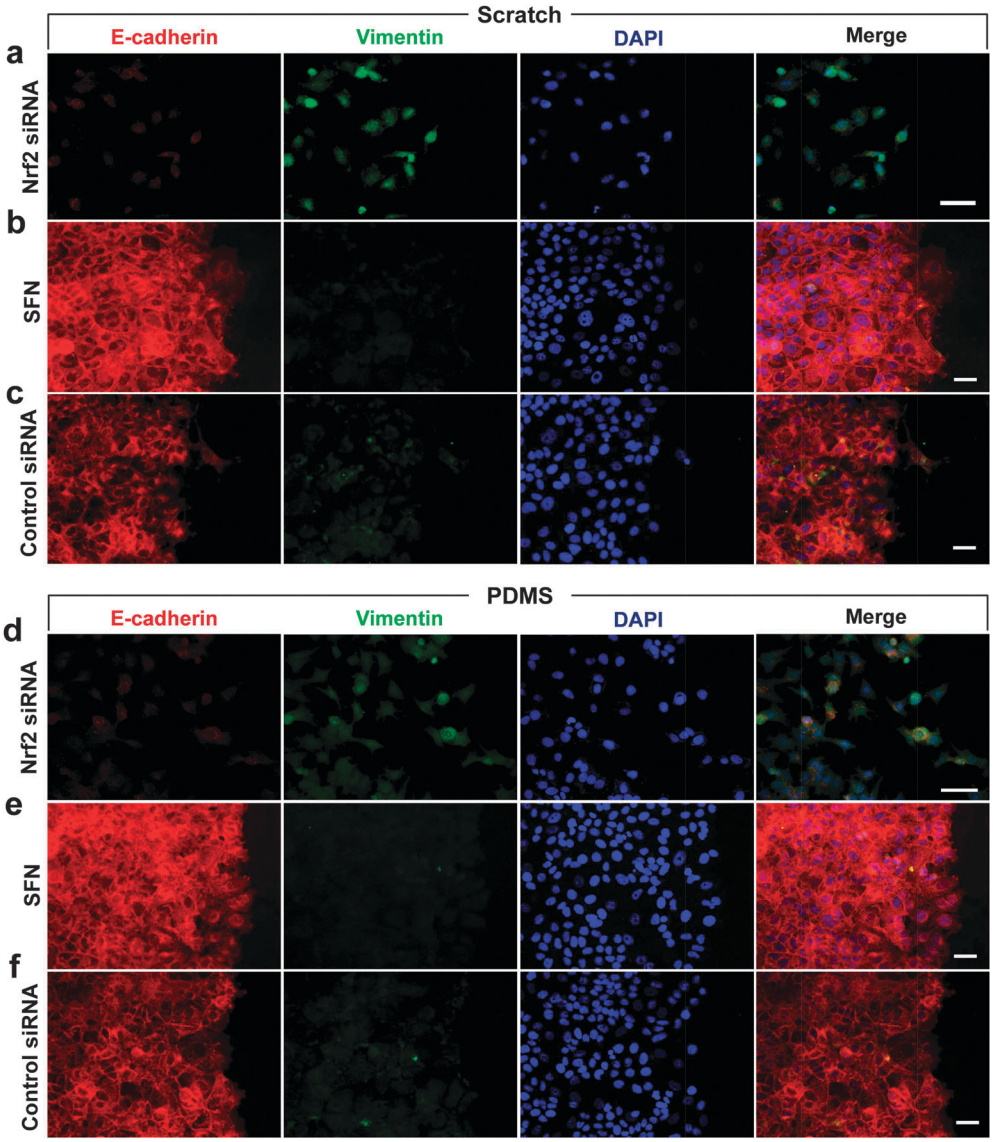

Fig. 8 Inhibitory role of Nrf2 in injury-induced EMT. The scratch (a–c) and PDMS (d–f) assays were performed to evaluate the cell behaviors with different treatments. (a,d) Cells transfected with Nrf2 siRNA. (b,e) Cells treated with 5.0 μM SFN. (c,f) Cells transfected with control siRNA. MCF7 cells were tested in the experiment. E-cadherin and vimentin were monitored in the cells. DAPI was used as counterstain. Scale bars, 50 μm.

near the wound, which maximize at the leading edge and decay in ~150 μm (Fig. 3). This length scale also correlates with the spatial distribution of ROS and Nrf2 near the wound. These results directly address a fundamental question in collective cell behavior: how many cells are actively responding to the injury and contributing to the collective cell response?[44,45] It is challenging to determine if the cell movement is driven passively from the leading edge or actively from the cells adjacent to the wound. Our single-cell analyses, on the other hand, determine the length scale involved in the collective cell response and show that cells far behind the leading edge actively respond to the injury. These results suggest spatial coordination among the cells during collective cell migration.

Another interesting implication of this study is the involvement of Nrf2 in the injury-induced cell response. In particular, we observed induction of ROS and *HO-1* mRNA that are regulated by Nrf2. To study the spatiotemporal distribution of Nrf2, a Nrf2-YFP stable cell line was developed and showed upregulation of the Nrf2 protein level near the wound edge. In the scratch assay, two Nrf2 waves were observed approximately 3 h and 24 h after wounding. Similarly, two-wave responses of mitogen-activated protein kinase (MAPK) after wounding have been reported in Madin-Darby canine kidney (MDCK) cells.[35,46] In these studies, the second MAPK wave was observed in the injury-free assay. In contrast, we did not observe Nrf2 elevation in the PDMS assay, suggesting that the Nrf2 and MAPK signaling may be regulated differently within the context of injury response. More importantly, both immunostaining, cell counting, and immunoblot results suggest that Nrf2 has an inhibitory effect on injury-induced EMT. Suppression of Nrf2 represses E-cadherin based cell–cell contact, induces mesenchymal biomarkers (*i.e.* vimentin, N-cadherin, Snail), detaches neighbouring cells,

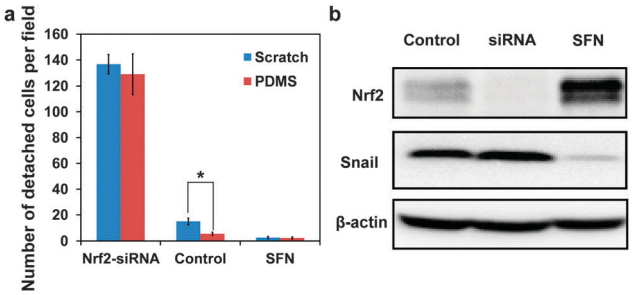

Fig. 9 Nrf2 has an inhibitory role in EMT. (a) Quantification of the number of detached cells in the PDMS and scratch assays. MCF7 cells were tested in the experiment. Control represents the PDMS and scratch assays with no treatment (* $P < 0.05$ compared between scratch and PDMS assays). (b) Nrf2 and Snail protein expressions with different treatments. Cells were transfected with 20 nM siRNA for 48 hours or treated by 5.0 μM SFN for 12 hours.

and increases cell migration. This is consistent with a recent study suggesting that the loss of Nrf2 in oncogenic cancer cells increases their propensity to migrate faster.[22] In contrast to the classical concept of an "all-or-nothing" switch, EMT is recently suggested to be a continuous spectrum of cell states.[11,12] Since injury also induces the Nrf2 activity, Nrf2 may serve as an autoregulatory mechanism to regulate EMT in a negative feedback loop to enable efficient migration of the cohesive epithelia (Fig. 10). Further mechanistic study is required to clarify the mechanism of how Nrf2 inhibits EMT and the regulation of injury-induced EMT. Unregulated or unwanted EMT has been associated with various pathological processes. The ability to modulate injury-induced EMT by targeting Nrf2 could potentially be a useful therapeutic approach for suppression of biopsy or surgery induced cancer metastasis and inhibition of fibrosis in injured tissues.[13–17]

Our results demonstrate that cell injury triggers a set of cellular injury responses. Nevertheless, the exact cellular mechanism that is responsible for injury sensing remains unclear. A contributory mechanism for the surviving cells to "sense" the injury is the release of intracellular contents in the extracellular space after wounding. ATP, for instance, can rapidly release from injured cells near the wound.[47] In fact, ATP is known to mediate ROS production and activates ROS-dependent oxidative stress response.[48] We have also confirmed that addition of extracellular ATP or cell lysate to epithelial cells can induce ROS (Fig. S8, ESI†). Diffusible factors, however, may not fully explain the injury sensing process and we do not rule out the possibility that release of contact inhibition is also necessary in injury sensing. In our experiment, initial ROS response is only observed in cells at the leading edge, which experience a release of contact inhibition. Additional sensing and intercellular communication mechanisms are likely involved in the injury sensing mechanism. For instance, cell injury induces calcium wave propagation near the wound and the calcium signal can communicate among the cells by extracellular chemical stimuli or intercellular signaling through cell–cell junctions.[49,50] In addition, cell traction force has also been suggested to induce the cell response.[46,51] Traction force microscopy has confirmed the involvement of cells well back from the leading edge in force generation.[52] Further systematic investigations are required to clarify these interrelated molecular and signaling events for elucidating the cellular injury sensing mechanisms.

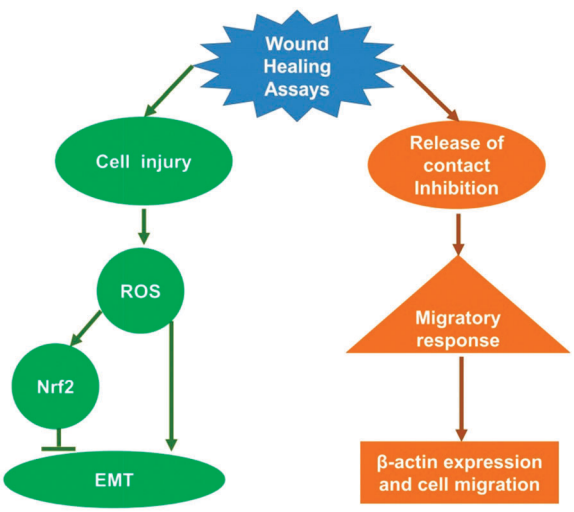

Fig. 10 Proposed modular cell responses and the Nrf2-EMT autoregulatory loop in injury-induced collective migration.

Conclusion

In summary, the study presented herein provides new insights into the coordinated, modular cell responses in injury-induced collective migration. Using the dsLNA probe, we demonstrate a novel approach to monitor intracellular gene expression in multicellular systems and directly determine the cells that are actively responding to the injury. Our results also suggest a potential autoregulatory role of Nrf2 in injury-induced EMT. These findings will lead to further investigations of the mechanistic basis of injury-induced cell responses and may underpin novel therapeutic strategies in the future.

Acknowledgements

The authors thank A. Rasmussen for critical reading of the manuscript and H. Wang for technical assistance in the Nrf2-YFP experiment. This work is supported by NIH Director's New Innovator Award (1DP2OD007161-01) and the National Cancer Institute (5R01CA154377-02).

Notes and references

1 P. Friedl and D. Gilmour, *Nat. Rev. Mol. Cell Biol.*, 2009, **10**, 445–457.
2 P. Rorth, *Annu. Rev. Cell Dev. Biol.*, 2009, **25**, 407–429.
3 R. Riahi, Y. L. Yang, D. D. Zhang and P. K. Wong, *J. Lab. Autom.*, 2012, **17**, 59–65.
4 E. N. Arwert, E. Hoste and F. M. Watt, *Nat. Rev. Cancer*, 2012, **12**, 170–180.

5 M. J. Slepian, S. P. Massia, B. Dehdashti, A. Fritz and L. Whitesell, *Circulation*, 1998, **97**, 1818–1827.
6 W. T. Gerthoffer, *Circ. Res.*, 2007, **100**, 607–621.
7 P. Friedl, J. Locker, E. Sahai and J. E. Segall, *Nat. Cell Biol.*, 2012, **14**, 777–783.
8 P. Friedl, *Curr. Opin. Cell Biol.*, 2004, **16**, 14–23.
9 R. Kalluri and R. A. Weinberg, *J. Clin. Invest.*, 2009, **119**, 1420–1428.
10 J. P. Thiery and J. P. Sleeman, *Nat. Rev. Mol. Cell Biol.*, 2006, **7**, 131–142.
11 C. Revenu and D. Gilmour, *Curr. Opin. Genet. Dev.*, 2009, **19**, 338–342.
12 D. S. Micalizzi, S. M. Farabaugh and H. L. Ford, *J. Mammary Gland Biol. Neoplasia*, 2010, **15**, 117–134.
13 R. Demicheli, M. W. Retsky, W. J. M. Hrushesky, M. Baum and I. D. Gukas, *Ann. Oncol.*, 2008, **19**, 1821–1828.
14 M. Retsky, R. Demicheli and W. Hrushesky, *Lancet*, 2001, **357**, 1048.
15 D. G. Baker, T. M. Masterson, R. Pace, W. C. Constable and H. Wanebo, *Surgery*, 1989, **106**, 525–532.
16 G. J. van der Bij, S. J. Oosterling, R. H. J. Beelen, S. Meijer, J. C. Coffey and M. van Egmond, *Ann. Surg.*, 2009, **249**, 727–734.
17 D. F. Alonso, G. V. Ripoll, J. Garona, N. B. Iannucci and D. E. Gomez, *Curr. Pharm. Biotechnol.*, 2011, **12**, 1974–1980.
18 M. Schafer and S. Werner, *Pharmacol. Res.*, 2008, **58**, 165–171.
19 Y. A. Huo, W. Y. Qiu, Q. Pan, Y. F. Yao, K. Y. Xing and M. F. Lou, *Exp. Eye Res.*, 2009, **89**, 876–886.
20 A. Lau, N. F. Villeneuve, Z. Sun, P. K. Wong and D. D. Zhang, *Pharmacol. Res.*, 2008, **58**, 262–270.
21 D. H. Shin, H. M. Park, K. A. Jung, H. G. Choi, J. A. Kim, D. D. Kim, S. G. Kim, K. W. Kang, S. K. Ku, T. W. Kensler and M. K. Kwak, *Free Radicals Biol. Med.*, 2010, **48**, 1051–1063.
22 G. Rachakonda, K. R. Sekhar, D. Jowhar, P. C. Samson, J. P. Wikswo, R. D. Beauchamp, P. K. Datta and M. L. Freeman, *Oncogene*, 2010, **29**, 3703–3714.
23 V. Sanchez-Freire, A. D. Ebert, T. Kalisky, S. R. Quake and J. C. Wu, *Nat. Protocols*, 2012, **7**, 829–838.
24 P. K. Wong, F. Q. Yu, A. Shahangian, G. H. Cheng, R. Sun and C. M. Ho, *Proc. Natl. Acad. Sci. U. S. A.*, 2008, **105**, 5105–5110.
25 V. Gidwani, R. Riahi, D. D. Zhang and P. K. Wong, *Analyst*, 2009, **134**, 1675–1681.
26 R. Riahi, K. E. Mach, R. Mohan, J. C. Liao and P. K. Wong, *Anal. Chem.*, 2011, **83**, 6349–6354.
27 D. Meserve, Z. Wang, D. D. Zhang and P. K. Wong, *Analyst*, 2008, **133**, 1013–1019.
28 R. Riahi, Z. Dean, T. H. Wu, M. A. Teitell, P. Y. Chiou, D. D. Zhang and P. K. Wong, *Analyst*, 2013, **138**, 4777–4785.
29 X. J. Wang, Z. Sun, N. F. Villeneuve, S. Zhang, F. Zhao, Y. Li, W. Chen, X. Yi, W. Zheng, G. T. Wondrak, P. K. Wong and D. D. Zhang, *Carcinogenesis*, 2008, **29**, 1235–1243.
30 D. M. Ren, N. F. Villeneuve, T. Jiang, T. D. Wu, A. Lau, H. A. Toppin and D. D. Zhang, *Proc. Natl. Acad. Sci. U. S. A.*, 2011, **108**, 1433–1438.
31 A. Lau, X. J. Wang, F. Zhao, N. F. Villeneuve, T. D. Wu, T. Jiang, Z. Sun, E. White and D. D. Zhang, *Mol. Cell. Biol.*, 2010, **30**, 3275–3285.
32 M. Poujade, E. Grasland-Mongrain, A. Hertzog, J. Jouanneau, P. Chavrier, B. Ladoux, A. Buguin and P. Silberzan, *Proc. Natl. Acad. Sci. U. S. A.*, 2007, **104**, 15988–15993.
33 E. Anon, X. Serra-Picamal, P. Hersen, N. C. Gauthier, M. P. Sheetz, X. Trepat and B. Ladoux, *Proc. Natl. Acad. Sci. U. S. A.*, 2012, **109**, 10891–10896.
34 E. R. Block, A. R. Matela, N. SundarRaj, E. R. Iszkula and J. K. Klarlund, *J. Biol. Chem.*, 2004, **279**, 24307–24312.
35 D. L. Nikolic, A. N. Boettiger, D. Bar-Sagi, J. D. Carbeck and S. Y. Shvartsman, *Am. J. Physiol.: Cell Physiol.*, 2006, **291**, C68–C75.
36 M. Zuker, *Nucleic Acids Res.*, 2003, **31**, 3406–3415.
37 N. Li and P. K. Wong, *Bioanalysis*, 2010, **2**, 1689–1699.
38 K. Wang, Z. Tang, C. J. Yang, Y. Kim, X. Fang, W. Li, Y. Wu, C. D. Medley, Z. Cao, J. Li, P. Colon, H. Lin and W. Tan, *Angew. Chem., Int. Ed.*, 2009, **48**, 856–870.
39 T. Jiang, Z. P. Huang, Y. F. Lin, Z. G. Zhang, D. Y. Fang and D. D. Zhang, *Diabetes*, 2010, **59**, 850–860.
40 H. Zheng, S. A. Whitman, W. Wu, G. T. Wondrak, P. K. Wong, D. Fang and D. D. Zhang, *Diabetes*, 2011, **60**, 3055–3066.
41 K. H. Lee and D. A. Cotanche, *Hear. Res.*, 1995, **87**, 9–15.
42 M. Atalay, N. Oksala, J. Lappalainen, D. E. Laaksonen, C. K. Sen and S. Roy, *Curr. Protein Pept. Sci.*, 2009, **10**, 85–95.
43 S. Mushtaq, Z. A. Naqvi, A. A. Siddiqui, C. Palmberg, J. Shafqat and N. Ahmed, *Proteomics*, 2007, **7**, 463–468.
44 R. Farooqui and G. Fenteany, *J. Cell Sci.*, 2005, **118**, 51–63.
45 G. Fenteany, P. A. Janmey and T. P. Stossel, *Curr. Biol.*, 2000, **10**, 831–838.
46 Y. Matsubayashi, M. Ebisuya, S. Honjoh and E. Nishida, *Curr. Biol.*, 2004, **14**, 731–735.
47 J. Yin, K. Xu, J. Zhang, A. Kumar and F. S. Yu, *J. Cell Sci.*, 2007, **120**, 815–825.
48 C. M. Cruz, A. Rinna, H. J. Forman, A. L. Ventura, P. M. Persechini and D. M. Ojcius, *J. Biol. Chem.*, 2007, **282**, 2871–2879.
49 P. J. Sammak, L. E. Hinman, P. O. T. Tran, M. D. Sjaastad and T. E. Machen, *J. Cell Sci.*, 1997, **110**, 465–475.
50 M. Junkin, Y. Lu, J. Long, P. A. Deymier, J. B. Hoying and P. K. Wong, *Biomaterials*, 2013, **34**, 2049–2056.
51 M. R. Ng, A. Besser, G. Danuser and J. S. Brugge, *J. Cell Biol.*, 2012, **199**, 545–563.
52 D. T. Tambe, C. C. Hardin, T. E. Angelini, K. Rajendran, C. Y. Park, X. Serra-Picamal, E. H. Zhou, M. H. Zaman, J. P. Butler, D. A. Weitz, J. J. Fredberg and X. Trepat, *Nat. Mater.*, 2011, **10**, 469–475.

